

Thermal stability of microstructural and optical modifications induced in sapphire by ultrafast laser filamentation

A. Benayas, D. Jaque, Ben McMillen, and K. P. Chen

Citation: *Journal of Applied Physics* **107**, 033522 (2010); doi: 10.1063/1.3280029

View online: <http://dx.doi.org/10.1063/1.3280029>

View Table of Contents: <http://scitation.aip.org/content/aip/journal/jap/107/3?ver=pdfcov>

Published by the [AIP Publishing](#)

Articles you may be interested in

Formation of optical barriers with excellent thermal stability in single-crystal sapphire by hydrogen ion implantation and thermal annealing

Appl. Phys. Lett. **99**, 111909 (2011); 10.1063/1.3637613

Microstructure evolution in carbon-ion implanted sapphire

J. Appl. Phys. **107**, 023508 (2010); 10.1063/1.3284963

Optical properties and structure characterization of sapphire after Ni ion implantation and annealing

J. Appl. Phys. **98**, 073524 (2005); 10.1063/1.2084314

Optical transmission through inelastically deformed shocked sapphire: stress and crystal orientation effects

J. Appl. Phys. **97**, 123529 (2005); 10.1063/1.1937470

Ordinary refractive index of sapphire in uniaxial tension and compression along the c axis

J. Appl. Phys. **93**, 1023 (2003); 10.1063/1.1530716



2014 Special Topics

PEROVSKITES

2D MATERIALS

MESOPOROUS MATERIALS

BIOMATERIALS/ BIOELECTRONICS

METAL-ORGANIC FRAMEWORK MATERIALS

Submit Today!

AIP | APL Materials

Thermal stability of microstructural and optical modifications induced in sapphire by ultrafast laser filamentation

A. Benayas,¹ D. Jaque,^{1,a)} Ben McMillen,² and K. P. Chen²

¹*Departamento de Física de Materiales C-IV, GIEL, Facultad de Ciencias, Universidad Autónoma de Madrid, 28049 Madrid, Spain*

²*Department of Electrical and Computer Engineering, University of Pittsburgh, Pittsburgh, Pennsylvania 15261, USA*

(Received 11 October 2009; accepted 1 December 2009; published online 9 February 2010)

We report on the thermal stability of both structural and optical micromodifications created by ultrafast laser written filaments in sapphire crystals. By using the Cr³⁺ traces as optical probes, we have concluded that the filaments are constituted by both *reversible* and *nonreversible* defects with very different spatial locations. The strain field measured from the analysis of R lines has been found to be erased at the same time when the reversible centers are recombined (~ 1100 °C). This fact seems to indicate that these defects act as *pinning centers* for the induced stress. Furthermore, we have found that the waveguide generated in the proximity of the filament disappear for annealing temperatures above 1100 °C. This clearly supports the assumption that waveguiding is produced by the strain stress induced refractive index increment based on the dominant electronic polarizability enhancement. © 2010 American Institute of Physics. [doi:10.1063/1.3280029]

I. INTRODUCTION

When a femtosecond laser pulse is tightly focused inside a crystalline lattice, nonlinear excitation processes from the valence to the conduction band are activated even in the case when the energy of incident photons is smaller than the band-gap energy.¹ Although the mechanisms at the basis of these nonlinear excitations are not yet well understood, the generation of well localized plasma at the focal volume is widely assumed.^{2,3} The presence of such well confined plasma drives the crystalline lattice to an extreme situation characterized by very high electronic temperatures and pressures.^{4–6} These extreme conditions produce, at the focal volume and in its surroundings, microstructural modifications that could remain after complete relaxation of the electronic subsystem.

The extension and nature of the permanent microstructural changes induced in the irradiated material depends on a large variety of conditions including irradiation parameters (pulse length, repetition rate, pulse energy, and polarization) as well as on the particular characteristics of the irradiated material. Among the different ultrafast inscribed microstructural modifications reported upto now in crystals and glasses, it is worth to be mentioned the compression/dilatation of the focal volume, changes in the crystalline orientation, changes in the spontaneous polarization, and changes in the local composition and local damage via optical breakdown.^{6–19} Any of these changes has its particular signature in the refractive index of the materials, in such a way that the refractive index is modified at the focal volume and surroundings. The magnitude of the refractive index modifications induced at the micro and submicroscale can range from 10^{-4} to 10^{-1} ,

allowing for the fabrication of photonics devices (such as waveguides and photonic crystals) in a large variety of materials including glasses and crystals.^{20–22}

Among the different crystals in which ultrafast laser inscription has been demonstrated, sapphire is of special relevance. It is regarded as one of the hardest crystals with a large Young's modulus (0.4 TPa) so that permanent structural modifications require very high energy confinements.⁷ In addition, it has been demonstrated that ultrafast laser-induced microstructural changes in sapphire are accompanied by relevant and smooth refractive index changes, which lead to light confinement in the surroundings of the focal spot of the ultrafast beam.²³ Based on these refractive index changes induced in the surroundings of focal volume and by translation of the sample during irradiation, channel buried waveguides have been fabricated with a great relevance as potential integrated laser sources and high temperature optical sensors.^{24–26} Nevertheless, and despite its interest from both fundamental and applied point of views, the time and thermal stability of the microstructural changes induced in the sapphire network (i.e., stability of the fabricated waveguides) after ultrafast laser inscription are still unexplored. This information is of relevance since it provides fundamental information about the physics beyond the ultrafast driven microstructural modifications and establishes the working limits of the fabricated photonic devices.

In this work, we have investigated the thermal stability of the microstructural changes induced in the sapphire systems after ultrafast laser irradiation. For this purpose, and based on the analysis of the microluminescence generated by Cr³⁺ traces, we have measured the spatial distribution of damage and stress in the surroundings of the ultrafast laser focal spot after different annealings at temperatures ranging from 100 to 1500 °C. From the analysis of these data, a distinction between reversible and nonreversible structural modifications, with a very different spatial distribution, has

^{a)}Electronic mail: daniel.jaque@uam.es.

been done. The waveguiding properties of the fabricated microstructures have been also systematically studied during the multistep annealing procedure. We have found that waveguiding was stable up to 1000 °C, this matching the annealing temperature that causes a total erasing of the reversible strain field created in the surroundings of the focal spot.

II. EXPERIMENTAL

The sample used in this work was a nominally pure sapphire crystal provided by Crystal Systems Inc. Fluorescence and absorption measurements revealed the presence of Cr³⁺ traces inside the crystal with an estimated concentration not larger than 0.1 at. %. Ultrafast laser irradiation was done by using a coherent MIRA oscillator and a RegA regenerative amplifier system. The output from the RegA was frequency doubled to produce 150 fs pulses at a wavelength of 385 nm and a repetition rate of 250 kHz. The writing beam was focused nominally into the sapphire sample at a depth of 150 μm with a 40× aspheric lens (numerical aperture =0.68). The sapphire sample was mounted on a three-axis motorized stage and translated at speeds ranging from 0.2 to 5 mm/s allowing inscription of damage filaments parallel to the A-axis (1120) crystallographic axis. Pulse energy was varied from 100 to 500 nJ. Repolishing of the end surface was done after the inscription process and before optical and structural analysis in order to remove any surface damage. After fabrication, the structures were annealed by placing the sample in an open atmosphere oven working up to 1500 °C.

Optical characterization of the damage filaments was done by using a conventional optical microscope working in transmission mode. The waveguiding properties of the fabricated filaments were analyzed by coupling a He-Ne beam (632 nm) parallel to the damage filaments by using a 10× microscope objective. The coupled light was collected from the exit face with a 40× microscope objective and imaged onto a charge-coupled device camera.

The spatial distribution of the microstructural changes induced in the surroundings of the inscribed filament was extracted from the analysis of the microfluorescence spectra generated by the Cr³⁺ traces. It consists of two intense narrow peaks located at 694.3 and 692.9 nm (shown in Fig. 1). These two narrow emissions are unequivocally related to the R lines of Cr³⁺ ions (the so-called R₁ and R₂) lines.²⁷ It is well known that the spectral positions of these two R lines are strongly influenced by the presence of compressive and tensile stress in the sapphire network. Indeed, the large pressure coefficients of these lines (−0.77 and −0.84 cm^{−1}/kbar for R₁ and R₂ lines, respectively) make them outstanding pressure sensors.²⁸ In addition to this, the intensity of these lines gives a measure of the local damage and presence of defects. As a consequence, the simultaneous analysis of the intensity and spectral position of these two fluorescence line provides information about the local damage and stress generated in the sapphire network. In order to extract this information with a submicrometric spatial resolution, the sample was placed in a scanning confocal microscope equipped with a 100× (0.9 numerical aperture) microscope objective which

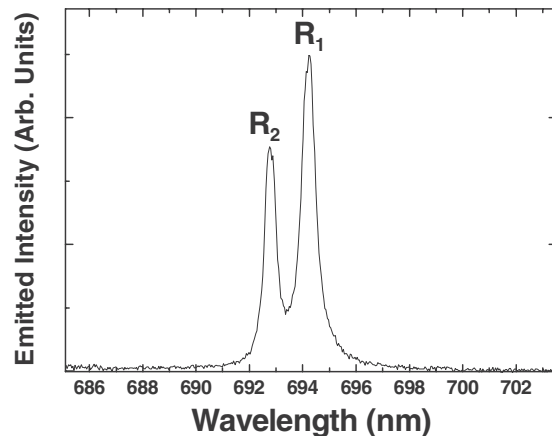


FIG. 1. Microluminescence spectrum generated from Cr³⁺ traces showing in detail the R lines which have been properly labeled.

focused the continuous wave 488 nm laser beam generated by an air cooled argon laser. The sapphire sample was orientated in such a way that the 488 nm beam propagates parallel to the laser inscribed filament, i.e., parallel to the A-axis (1120) crystallographic axis. The same objective was used for the collection of the Cr³⁺ luminescence. After passing through a confocal aperture, this fluorescence was focused into a fiber connected to a high resolution spectrometer. The sample was mounted on a XY motorized stage with a nominal resolution of 100 nm. This allows us to scan the 488 nm excitation spot over the transverse cross section of the laser inscribed filament.

III. RESULTS AND DISCUSSION

A. Thermal resistance of microstructural induced modifications

Figure 2(a) shows the optical microscope cross section image of the as-fabricated laser-induced modification produced in the sapphire sample with a pulse energy of 500 nJ

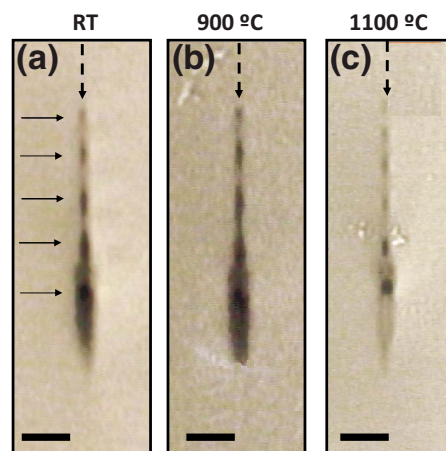


FIG. 2. (Color online) Optical transmission pictures of the end face of the sapphire sample irradiated with 500 nJ pulse energy and by translating the sample at 2 mm/s. Dashed arrows indicate the propagation direction of UV pulses. Solid arrows indicate the position of the self-focused spots. (a) Corresponds to the as-fabricated structure. (b) and (c) were obtained after 1 h annealing at 900 and 1100 °C, respectively. Scale bar is 20 μm and aspect ratio is 1:1.

with a translation speed of 0.2 mm/s (these writing conditions lead to the highest optical contrast). The propagation direction of the UV irradiation pulses is indicated by the dashed arrows. It is clear that ultrafast laser inscription has been created a modified area along the laser path, which extends over almost 60 μm . This modified area is clearly inhomogeneous as it is constituted by five distinct modified zones (hereafter referred as spots), which have been indicated by solid arrows. These five spots are quasiperiodically spaced and this suggests that they are self-formed by the balance of plasma defocusing from a previous formed spot and self-focusing of the laser pulses in the bulk medium, such as reported, for example, in CaF_2 and lithium niobate crystals.^{29,30} Although these spots lead to the highest optical contrast, some weaker darkening regions are also observed between these spots and in their surroundings. This suggests that in the as-fabricated structure the material has been strongly modified by the laser irradiation at the self-focused spots. Somewhat weaker structure modifications also occurs around self-focused spots. Figure 2(b) shows the optical transmission microscope image after 1 h annealing at 900 °C, showing not relevant changes in respect to the image obtained from the as-fabricated structure. Nevertheless, when the structure is annealed at 1100 °C a drastic change is observed [see Fig. 2(c)]. In this case, the optical contrast is only generated at the self-focused spots and it seems that the modification induced in their surroundings and between them has been almost erased.

Further understanding of data included in Fig. 2 can be obtained when the spatial distribution of the Cr^{3+} luminescence intensity is analyzed. The Cr^{3+} luminescence intensity is obtained by integrating emissions from both R lines. Figure 3 shows (top line) the spatial distribution of the Cr^{3+} luminescence intensity over the filament's cross section as obtained for the as-fabricated structure and after 1 h annealing at 900 and 1100 °C. It is clear that in the as-fabricated structure an almost continuous reduction of the Cr^{3+} luminescence has been obtained along the damage filament. This continuous luminescence reduction becomes more localized and discrete as the annealing temperature is increased. Indeed, when the annealing temperature reaches 1100 °C, the Cr^{3+} luminescence is only reduced at well-defined five locations, which matches with the location of the self-focused spots (indicated by shadow arrows). This temperature induced localization of the Cr^{3+} intensity reduction is even more noticeable when the intensity profiles obtained along the pulse path are plotted for the as-fabricated structure and after 1100 °C annealing (see bottom of Fig. 3). As mentioned above, in a first order approximation the reduction in the Cr^{3+} fluorescence efficiency can be associated with the presence of a large density of defects that act as quenching centers.³¹ Thus, data of Fig. 3 reveal that two different kinds of defects have been created along the pulse path.

- (1) Thermally removable defects induced in the surroundings of the self-focused spots. These defects were found to be completely recombined for annealing temperatures above 1100 °C.
- (2) Nonremovable centers created at the self-focused spots.

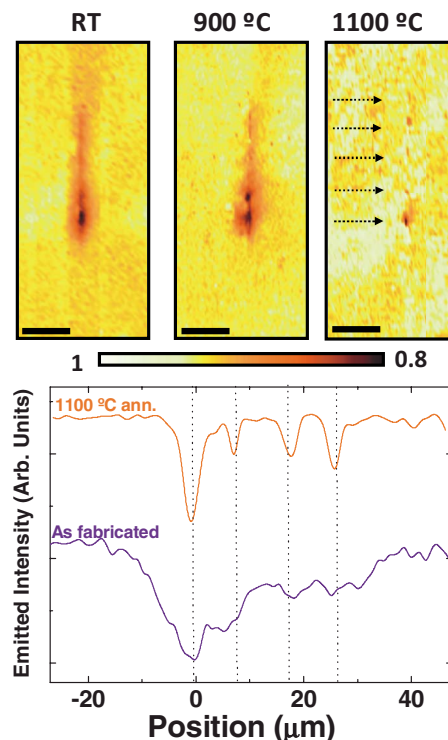


FIG. 3. (Color online) Top: Spatial distribution of the Cr^{3+} luminescence intensity as obtained from the damage filament obtained with a pulse energy of 500 nJ and 0.2 mm/s translation speed for different annealing temperatures. Dashed arrows indicate the spatial location of the self-focused spots. Bottom - Intensity profile obtained along the pulse path for the as-fabricated filament and after annealing for 1 h at 1100 °C. Vertical dashed lines indicate the spatial location of the self-focused spot.

These defects were found to be resistant upto the maximum temperature annealing studied in this work of 1500 °C. Due to their high thermal resistance, these defects are tentatively related to local optical breakdown of the sapphire network caused by the achievement of high photon densities during the pulse propagation.

The simultaneous presence of these two kinds of defects seems to be a general effect of ultrafast laser inscription in crystalline media. Indeed, for the particular case of neodymium doped yttrium aluminum garnet, it has been reported that femtosecond filaments are constituted by a well localized central core characterized by an irreversible damage surrounded by a somehow extended volume characterized by a large density of nonpermanent (thermally removable) defects.¹⁵

It is known from previous works that, in addition to defects, ultrafast laser inscription in sapphire also leads to the appearance of residual stress at the focal spot and in its surroundings.¹⁷ As it has been explained in Sec. II, the analysis of the Cr^{3+} luminescence allows for a direct measurement of the stress maps by just using the induced spectral shifts and the pressure coefficients of R lines. Figure 4 shows the spatial distribution of the residual stress generated in the sapphire crystal after ultrafast laser inscription corresponding to the damage filament obtained after irradiation with 500 nJ pulses and 0.2 mm/s translation speed.

The strain field generated in the as-fabricated structure is characterized by a compressive stress at the main spot and a

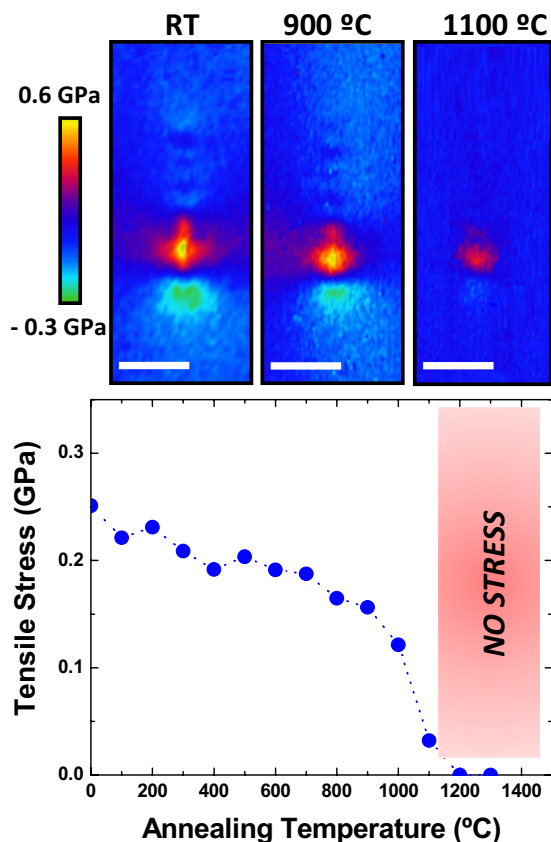


FIG. 4. (Color online) Top : Strain fields generated by the inscription of a damage filament in a sapphire crystal with a pulse energy of 500 nJ and 0.2 mm/s translation speed for different annealing temperatures. Bottom - Maximum tensile stress induced in the filament's surroundings as a function of the annealing temperature.

tensile stress just below it. Although weak, some periodic modulation in the induced stress can be observed above the main focal spot, which can be attributed again to the periodic self-focusing/defocusing of the laser pulses. In Fig. 4, we have also included the stress maps obtained after annealing for 1 h at 900 and 1100 °C. It is clear from the top images of Fig. 4 that thermal annealing of the structure causes a reduction in the strain field. Indeed, when the structure is annealed above 1100 °C, only relevant stress is measured at the main focal spot whereas the tensile stress area is almost erased. The change in the strain field has been found to be nonmonotonous. In order to illustrate this fact, the maximum tensile stress generated below the main focal spot has been plotted as a function of the annealing temperature (see bottom graph in Fig. 4). In the temperature range between 100 and 1000 °C the induced tensile stress slightly reduces with temperature continuously. For temperatures above 1000 °C this trend suddenly changes. In the 1000–1200 °C temperature range the maximum residual tensile stress is drastically reduced. Similar behavior has been found when the maximum compressive stress induced at the main focal spot has been analyzed. It is worth to note at this point that this temperature range well matches with the recombination temperature of the removable defects suggesting that these defects act as pinning centers for the strain field. Once these *pinning* defects were recombined, a complete elastic relaxation of the sapphire network is undergone. This pinning effect can be

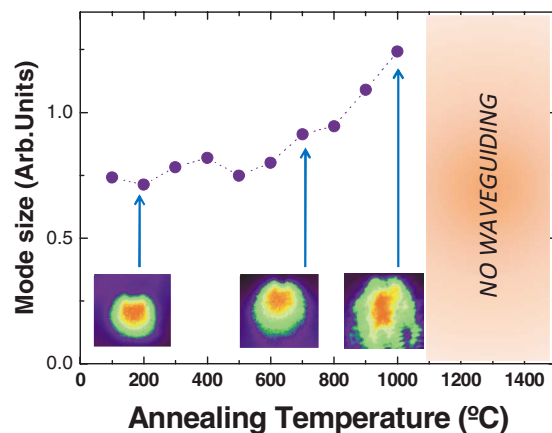


FIG. 5. (Color online) Size of waveguide's propagation mode at 632 nm for different annealing temperatures. Insets show the waveguide's propagation mode at 632 nm for three different temperatures.

explained in terms of the fact that the density fluctuations and slight ionic rearrangements inherent to defects avoids a complete elastic relaxation of the lattice.

B. Thermal resistance of waveguiding

Previous studies have demonstrated that waveguiding occurs in the surroundings of ultrafast laser inscribed filaments in sapphire.²³ In the particular case of the filament under study in this work (500 nJ pulse energy and 2 mm/s translation speed), waveguiding has been found to occur just below the main focal spot, where a local dilatation of the sapphire network has been produced (according to the stress maps of Fig. 4). This agrees with previous works reporting on an unexpected refractive index increment when the sapphire network is dilated and it has been explained in terms of the dominant increment in the electronic polarizability over the density decrease.³² If previous assumptions were correct then the waveguide is expected to disappear once the crystalline network overcome a complete elastic relaxation so that the strain field is erased (and so the refractive index increment). In order to check this, the waveguiding properties of the damage filament have been investigated after different annealing temperatures. Results have been summarized in Fig. 5 in which we show the average waveguide mode size as obtained for different annealing temperatures. Insets show the measured waveguide modes from which the average size was calculated. From this figure, it is clear that in the 100–1000 °C the size of the waveguide's mode increases monotonously with the annealing temperature. This suggests a monotonous reduction in the refractive index contrast. This is, indeed, in agreement with the monotonous decrease in the tensile strain observed in this temperature range (see Fig. 4). Furthermore, no waveguiding was observed for annealing temperatures above 1100 °C indicating that the initially induced refractive index increment has been completely erased. This agrees with the complete removal of the sapphire dilatation (i.e., of the tensile stress) that takes place at this temperature (see Fig. 4). Thus, the comparison between the experimental data included in Figs. 4 and 5 unequivocally indicate that the mechanism of refractive index

increment responsible of waveguiding is the local dilatation of the sapphire network produced in the surroundings of the focal spot.

It is well-known that photosensitivity induced by ultrafast laser radiation irradiation have been observed in a wide array of transparent materials. It should be pointed out that the erasing temperature for the optical modifications in sapphire reported in this paper (>1000 °C) is similar to the erasing temperature previously reported for other optical devices fabricated by the ultrafast laser radiation such as high-temperature stable fiber Bragg gratings in fibers.^{33–36} This paper provides circumstantial evidence that the universal photosensitivity response induced by the ultrafast laser could share common mechanisms.

IV. CONCLUSIONS

In summary, we have investigated the thermal stability of both structural and optical modifications induced by ultrafast laser filamentation in sapphire crystals. By using the Cr^{3+} traces as optical probes, we have concluded that two different types of defects have been created by the ultrafast laser filamentation. These two defects are differentiated by their different resistance against thermal induced recombination. In those areas where femtosecond pulses have been self-focused optical break-down a high density of nonremovable defects is induced pointing out a well spatial localized permanent optical break-down of the sapphire lattice. The surroundings of these permanently damaged area are characterized by a high density of nonpermanent defects that are recombined when the lattice is heated above 1000 °C. This temperature has been found not to be critical only for defect recombination but also for the complete erasing of the residual stress induced in the surroundings of the filamentation damaged area. The simultaneous defect recombination and stress relaxation seems to indicate that the nonpermanent defects act as stress pinning centers. Finally, we have found that waveguiding in the proximity of the filamentation damage track is completely removed when the tensile stress is thermally relaxed, i.e., for annealing temperatures above 1000 °C. This establishes the operation limit of these waveguides and also evidenced that the waveguiding mechanism is the dilatation induced refractive index increment originated in the surroundings of the filament damage track.

Thus, this work provides a new understanding of the physics below the modification of an extremely hard material (sapphire) by ultrafast laser inscription, this being of high fundamental interest. In addition we have established the operation limits of sapphire ultrafast laser inscribed buried waveguides, this information of high practical relevance.

ACKNOWLEDGMENTS

This work has been supported by the Universidad Autónoma de Madrid ad Comunidad Autónoma de Madrid (Project No. CCG08-UAM/MAT-4434), by the Spanish Ministerio de Educación y Ciencia (Grant No. MAT 2007-64686), and by the National Science Foundation of the U.S.

(Grant No. CMMI0900564).

- ¹S. S. Mao, F. Quere, S. Guizard, X. Mão, R. E. Russo, G. Petite, and P. Martin, *Appl. Phys. A: Mater. Sci. Process.* **79**, 1695 (2004).
- ²W. Gawelda, D. Puerto, J. Siegel, A. Ferrer, A. Ruiz de la Cruz, H. Fernandez, and J. Solis, *Appl. Phys. Lett.* **93**, 121109 (2008).
- ³E. Gamaly, S. Juodkazis, K. Nishimura, H. Misawa, and B. Luther-Davis, *Phys. Rev. B* **73**, 214101 (2006).
- ⁴N. Bloembergen, *IEEE J. Quantum Electron.* **10**, 375 (1974).
- ⁵B. C. Stuart, M. D. Feit, A. M. Rubenchik, B. W. Shore, and M. D. Perry, *Phys. Rev. Lett.* **74**, 2248 (1995).
- ⁶C. B. Schaffer, J. F. García, and E. Mazur, *Appl. Phys. A: Mater. Sci. Process.* **76**, 351 (2003).
- ⁷S. Juodkazis, K. Nishimura, S. Tanaka, H. Misawa, E. G. Gamaly, B. Luther-Davis, L. Hallo, P. Nicolai, and V. T. Tikhonchuk, *Phys. Rev. Lett.* **96**, 166101 (2006).
- ⁸C. Méndez, J. R. Vazquez de Aldana, G. A. Torchia, and L. Roso, *Appl. Phys. B: Lasers Opt.* **86**, 343 (2007).
- ⁹A. M. Streltsov and N. Borrelli, *J. Opt. Soc. Am. B* **19**, 2496 (2002).
- ¹⁰F. Vega, J. Armengol, V. Diez-Blanco, J. Siegel, J. Solis, B. Barcones, A. Perez-Rodriguez, and L. Loza-Alvarez, *Appl. Phys. Lett.* **87**, 021109 (2005).
- ¹¹J. Burghoff, C. Grebin, S. Nolte, and A. Tünnermann, *Appl. Surf. Sci.* **253**, 7899 (2007).
- ¹²R. R. Thomson, S. Campbell, I. J. Blewett, A. K. Kar, and D. T. Reid, *Appl. Phys. Lett.* **88**, 111109 (2006).
- ¹³R. Osellame, G. Della Valle, N. Chiodo, S. Taccheo, P. Laporta, O. Svelto, and G. Cerullo, *Appl. Phys. A: Mater. Sci. Process.* **93**, 17 (2008).
- ¹⁴A. Ródenas, J. A. Sanz García, D. Jaque, G. A. Torchia, C. Méndez, I. Arias, L. Roso, and F. Agulló-Rueda, *J. Appl. Phys.* **100**, 033521 (2006).
- ¹⁵A. Ródenas, G. A. Torchia, G. Lifante, E. Cantelar, J. Lamela, F. Jaque, L. Roso, and D. Jaque, *Appl. Phys. B: Lasers Opt.* **95**, 85 (2009).
- ¹⁶D. C. Deshpande, A. P. Malshe, E. A. Stach, V. Radmilovic, D. Alexander, D. Doerr, and D. Hirt, *J. Appl. Phys.* **97**, 074316 (2005).
- ¹⁷A. Ródenas, L. M. Maestro, M. O. Ramírez, G. A. Torchia, L. Roso, F. Chen, and D. Jaque, *J. Appl. Phys.* **106**, 013110 (2009).
- ¹⁸C. B. Schaffer, A. O. Jamison, and E. Mazur, *Appl. Phys. Lett.* **84**, 1441 (2004).
- ¹⁹G. Zhou and M. Gu, *Appl. Phys. Lett.* **87**, 241107 (2005).
- ²⁰S. Juodkazis, V. Mizeikis, and H. Misawa, *J. Appl. Phys.* **106**, 051101 (2009).
- ²¹G. Zhou and M. Gu, *Opt. Lett.* **31**, 2783 (2006).
- ²²R. Osellame, M. Lobino, N. Chiodo, M. Marangoni, G. Cerullo, R. Ramponi, H. T. Bookey, R. R. Thomson, N. D. Psaila, and A. K. Kar, *Appl. Phys. Lett.* **90**, 241107 (2007).
- ²³A. Benayas, D. Jaque, B. McMillen, and K. P. Chen, *Opt. Express* **17**, 10076 (2009).
- ²⁴Y. Zhang, G. Pickrell, B. Qi, A. Safaai-Jazi, and A. Wang, *Opt. Eng.* **43**, 157 (2004).
- ²⁵J. H. Kim, M.-K. Chen, C. E. Yang, J. Lee, S. S. Yin, P. Ruffin, E. Edwards, C. Brantley, and C. Luo, *Opt. Express* **16**, 4085 (2008).
- ²⁶V. Apostolopoulos, L. M. B. Hickey, D. A. Sager, and J. S. Wilkinson, *Opt. Lett.* **26**, 1586 (2001).
- ²⁷R. A. Forman, G. J. Piermarini, J. D. Barnett, and S. Block, *Science* **176**, 284 (1972).
- ²⁸Q. Ma and D. R. Clarke, *J. Am. Ceram. Soc.* **76**, 1433 (1993).
- ²⁹X. Hu, Y. Dai, L. Yang, J. Song, C. Zhu, and J. Qiu, *J. Appl. Phys.* **101**, 023112 (2007).
- ³⁰A. Ródenas, A. H. Nejadmalayeri, D. Jaque, and P. Herman, *Opt. Express* **16**, 13979 (2008).
- ³¹B. Henderson and G. F. Imbusch, *Optical Spectroscopy of Inorganic Solids* (Oxford Science, New York, 1989).
- ³²S. C. Jones, B. A. M. Vaughan, and Y. M. Gupta, *J. Appl. Phys.* **90**, 4990 (2001).
- ³³O. V. Butov, E. M. Dianov, and K. M. Golant, *Meas. Sci. Technol.* **17**, 975 (2006).
- ³⁴A. Saliminia, N. T. Nguyen, S. L. Chin, and R. Vallée, *J. Appl. Phys.* **99**, 093104 (2006).
- ³⁵Y. Li, C. R. Liao, D. N. Wang, T. Sun, and K. T. V. Grattan, *Opt. Express* **16**, 21239 (2008).
- ³⁶B. Zhang and M. Kahrizi, *IEEE Sens. J.* **7**, 586 (2007).